SUPPORTING INFORMATION

Mechanistic Insights into Crossover-Dependent Nuclease Resistance of PX vs. dsDNA using Enhanced Sampling

Sandip Mandal,[†] Arun Richard Chandrasekaran,[‡] and Prabal K. Maiti[*,†]

†*Center for Condensed Matter Theory, Department of Physics, Indian Institute of Science, Bangalore 560012, India*

‡*The RNA Institute, University at Albany, State University of New York, Albany, NY, 12222, USA*

E-mail: maiti@iisc.ac.in

Phone: +91-80-2293-2865. Fax: +91-80-2360-2602

S.1 MD simulation conformations of Juxtaposed-DNA; JX's (JX1-JX4) in the presence of 150 mM monovalent NaCl ions

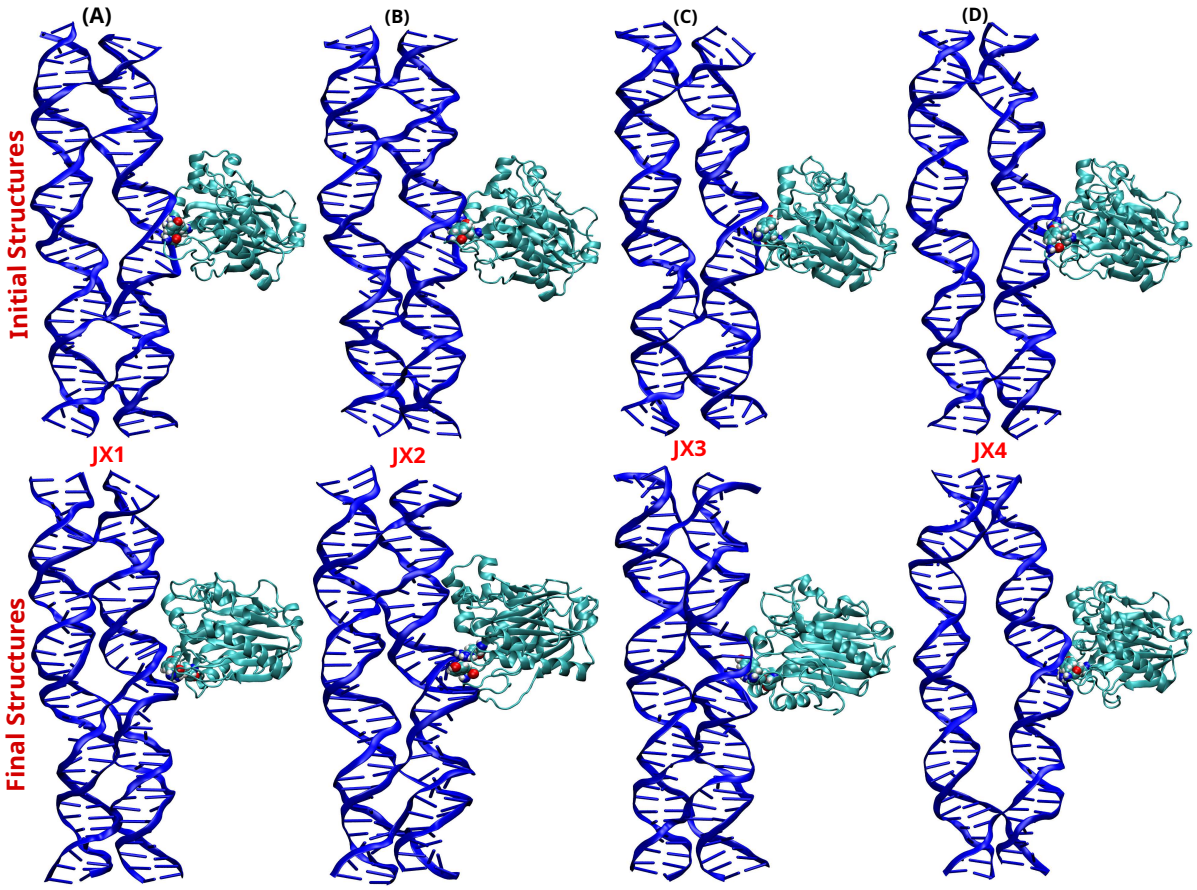

Figure S.1: Representations of instantaneous conformations of the four juxtaposed topoisomers of PX-DNA, as JX1, JX2, JX3, and JX4; by removing 1, 2, 3, and 4 crossover points in PX-DNA structure, in the presence of 150 mM monovalent NaCl ions. (A-B) The upper panel shows the initial conformations of JX-DNase I complexes, where DNase I enzymes COM are positioned ∼26 Å away from the nearest DNA duplexes COM. The lower panel depicts conformations from the final frames of the 300 ns MD simulations. With decreasing crossover points (JX1-JX4), DNase I binding affinity progressively increases due to enhanced structural flexibility and widened minor grooves, which provide sufficient space for the enzyme to grip the DNA grooves.

S.2 Instantaneous MD simulation conformations of ds-DNA and PX-DNA in the presence of divalent cations

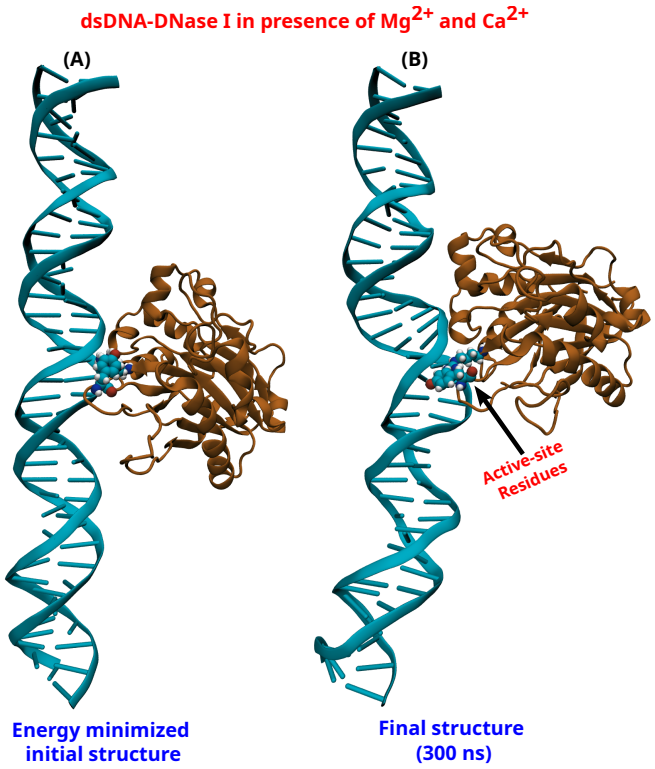

Figure S.2: Instantaneous snapshots of the - (A) Initial conformations of the dsDNA-DNase I complex, in which the center of mass (COM) of DNase I nuclease was positioned ∼26 Å away from the COM of the nearest DNA duplex. (B) The right panel shows representative conformations from the final frames of the 300 ns molecular dynamics simulations in the presence of 10 mM divalent Mg^{2+} and Ca^{2+} ions. The van der Waals (vdW) spheres highlight the active-site residues of DNase I. For clarity, water molecules and ions are omitted.

The instantaneous energy-minimized initial and final structures of the dsDNA-DNase I complex are shown in Figure S.2A and S.2B, respectively. The final conformation at 300 ns reveals that DNase I nuclease binds strongly within the minor groove of dsDNA in presence of divalent Mg^{2+} and Ca^{2+} cations, adopting binding conformations similar to those observed in simulations with only Na^{+} ions. Figures S.3A and S.3B present the corresponding initial and final structures of the PX-DNase I complex. Interestingly, in the presence of Mg^{2+}/Ca^{2+} ions, the active-site residues R41 and Y76 (as shown in vdW spheres) exhibit enhanced and

more closer interactions with the PX-DNA minor grooves, which were not observed in the presence of only Na^+ ions. Additionally, the presence of divalent cations increases the flexibility of both dsDNA and PX motifs relative to Na^+ conditions, as evidenced by their reduced stretch modulus values as reported in Table St.5 and Table St.6.

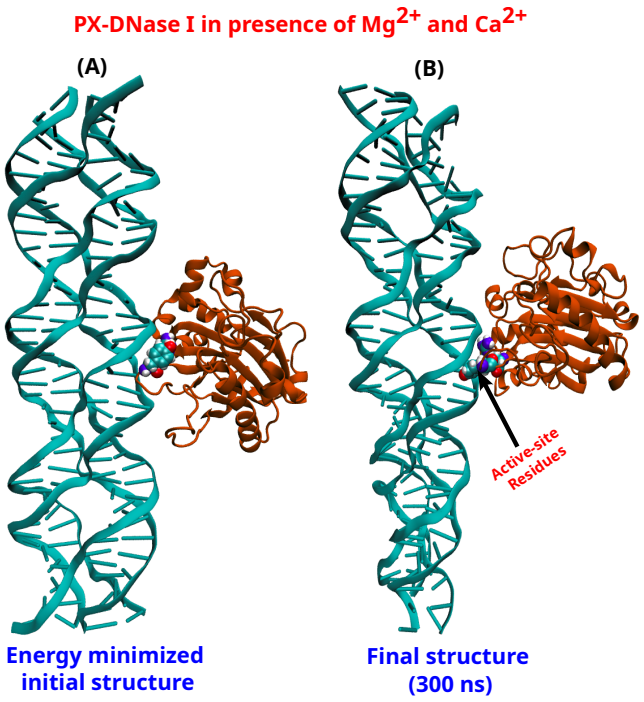

Figure S.3: (A) Initial conformations of the PX-DNase I complex, in which the center of mass (COM) of DNase I nuclease was positioned ∼26 Å away from the COM of the nearest DNA duplex of the PX-DNase I system. (B) The right panel shows representative conformations from the final frames of the 300 ns molecular dynamics simulations. The van der Waals (vdW) spheres highlight the active-site residues of the DNase I nuclease.

S.3 Number of Hydrogen Bond Counts

Table St.1: **Time-averaged number of hydrogen bonds at 300 K using the final 100 ns from the 300 ns MD simulation trajectory for all six DNA-DNase I complexes in the presence of 150 mM NaCl ions.**

System	Number of H-bonds
dsDNA	6.89±1.77
JX4	5.74±2.16
JX3	5.72±2.0
JX2	4.02±1.84
JX1	5.24±2.16
PX	3.13±1.77

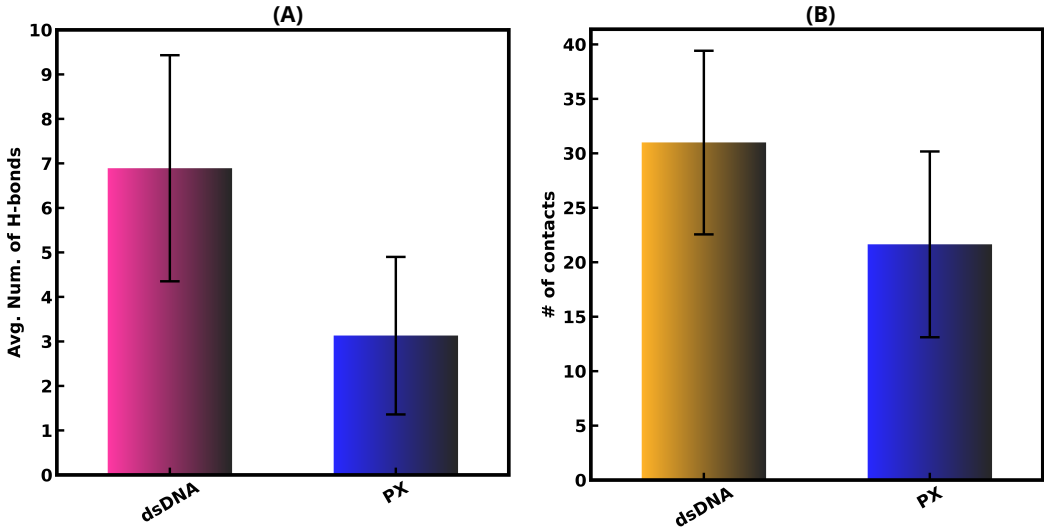

Figure S.4: Statistics of hydrogen bonds between DNA nanostructures and DNase I nuclease via bar plots, in the presence of 150 mM NaCl ions.

S.4 Minimum distance-based contact maps in the presence of divalent Mg^{2+} and Ca^{2+} ions

In order to identify the residues involved in the DNA-DNase I nuclease binding at close proximity, we have plotted minimum distance-based residue-residue contact maps for both dsDNA and PX-DNA residues with DNase I residues. The deep red-colored regions suggest residues in close contact within 10 Å minimum distance. As the active-site residues are mainly responsible for cleavage activity, we have considered a range of DNase I residues near the active site. The range of residues along the x-axis, with deep-red regions, will indicate which DNA residues exhibit the dominant binding propensity.

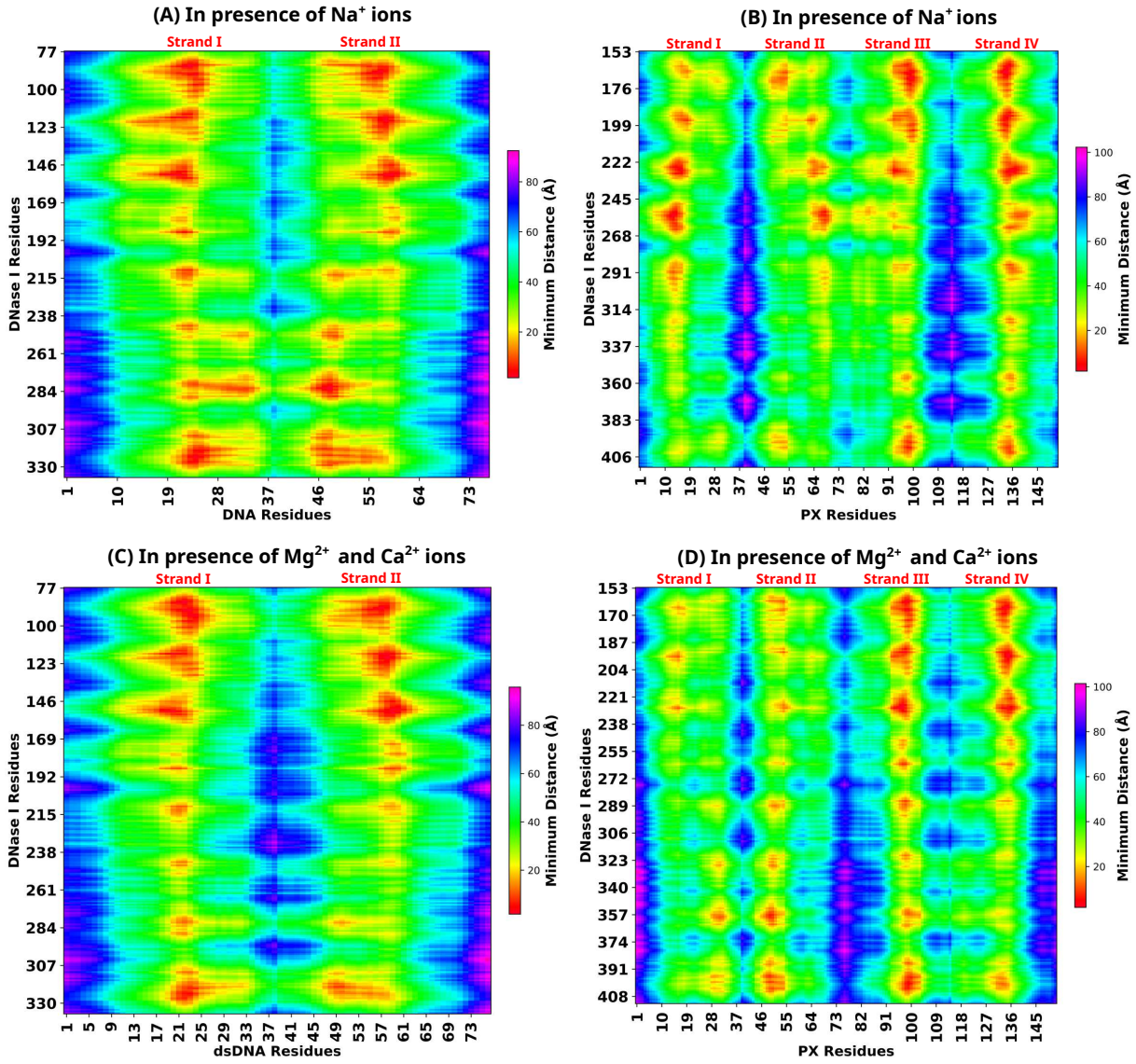

Figure S.5: Minimum distance-based contact maps highlighting interactions between all the DNA-motif and DNase I residues. Panels (A) and (B) show contact maps for dsDNA and PX in the presence of 150 mM Na^{+}, while panel (C) and (D) presents the corresponding contact maps for 10 mM Mg^{2+} and 10 mM Ca^{2+} ions, along 150 mM NaCl. The color bar denotes minimum distances (Å), with deep red colors indicating strong interactions ($<$ 10 Å), followed by yellow, green, and blue representing progressively larger distances.

Interactions involving the key DNase I active-site residues, particularly R41 and Y76, are central to nuclease activity and cannot be fully captured by global hydrogen-bond and number of contact analysis alone. Accordingly, we performed a detailed residue-level analysis focusing on active-site residues R41 and Y76 and quantified their close contacts with DNA

backbones in both the dsDNA and PX-DNA systems, as shown in Figure S.5.

To compare binding mechanisms, minimum distance-based contact maps were computed using the final 10 ns of the 300 ns trajectories (Figure S.5). The dsDNA-DNase I complex shows two x-axis regions corresponding to the two strands, whereas PX-DNA shows four regions representing its four strands. As shown in Figures S.5A and S.5B, ds-DNA forms strong contacts with eight DNase I residue regions (< 10 Å), while PX-DNA exhibits markedly weaker interactions, particularly with strands I-III (> 10 Å), indicating reduced binding under monovalent Na^+ conditions.

In the presence of divalent ions, DNA-DNase I interactions become stronger and highly localized (Figures S.5C and S.5D). While dsDNA shows stable contacts across both strands within the upper four DNase I residue regions, PX-DNA exhibits strong interactions only with strands III and IV, with minimal binding to strands I and II. This indicates preferential binding of DNase I to the nearest PX-DNA duplex, mediated by active-site and minor groove residues and stabilized by divalent cations.

To assess the role of divalent cations (Mg^{2+} and Ca^{2+}) in DNA-DNase I binding, we computed the radial distribution function, g(r), to quantify preferential localization of these cations in close proximity to the DNA backbone and DNase I atoms. The spatial distributions of the cations in the simulation box are shown in Figures S.6A and S.6B (Water and Na^+ ions are not shown for clarity).

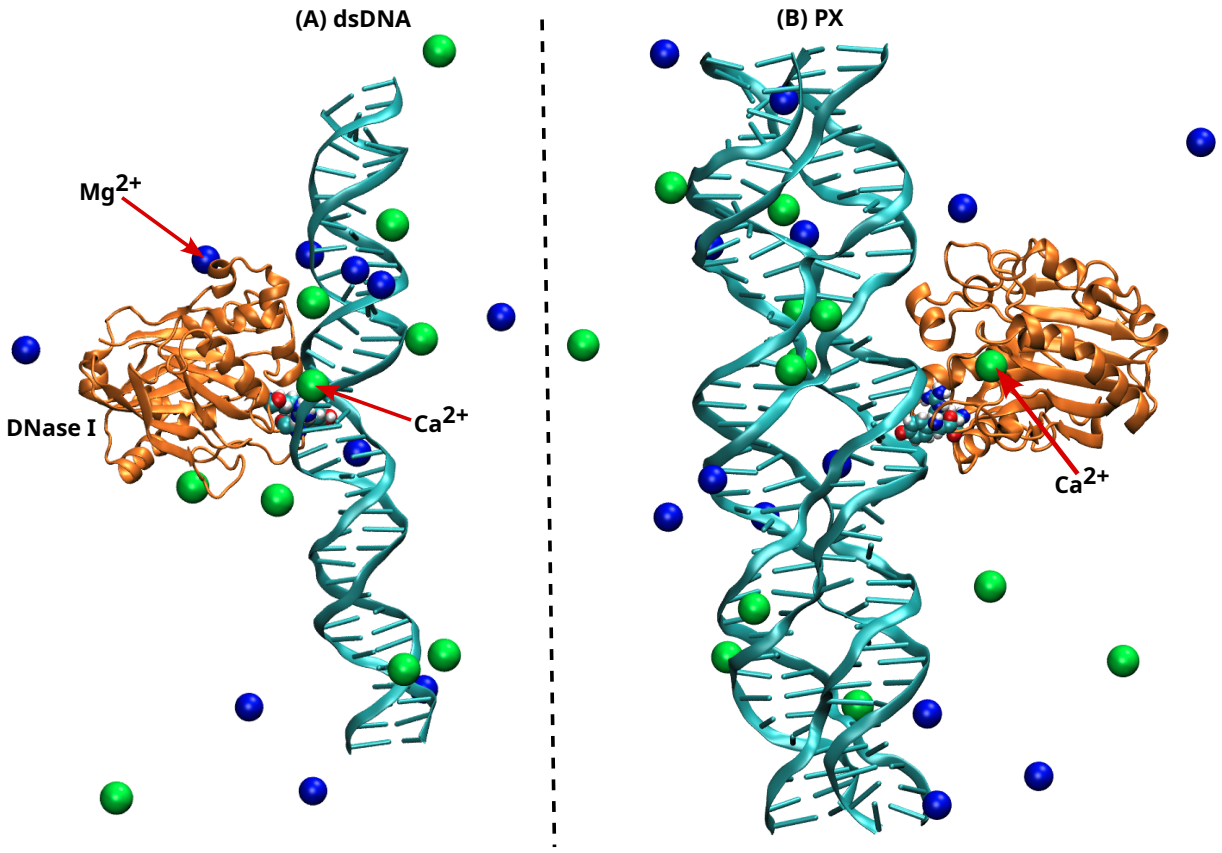

Figure S.6: Instantaneous snapshots of the dsDNA-DNase I complex showing (A) dsDNA-DNase I and (B) PX-DNase I conformations obtained from 300 ns all-atom molecular dynamics simulations in the presence of divalent Mg^{2+} (blue sphere) and Ca^{2+} (green sphere) ions. For clarity, water molecules and Na+ ions are omitted. The vdW spheres highlight the DNase I active-site residues R41 and Y76. The Ca^{2+} cation in green, shown by the arrow, stays bound throughout the last 100 ns of the simulation.

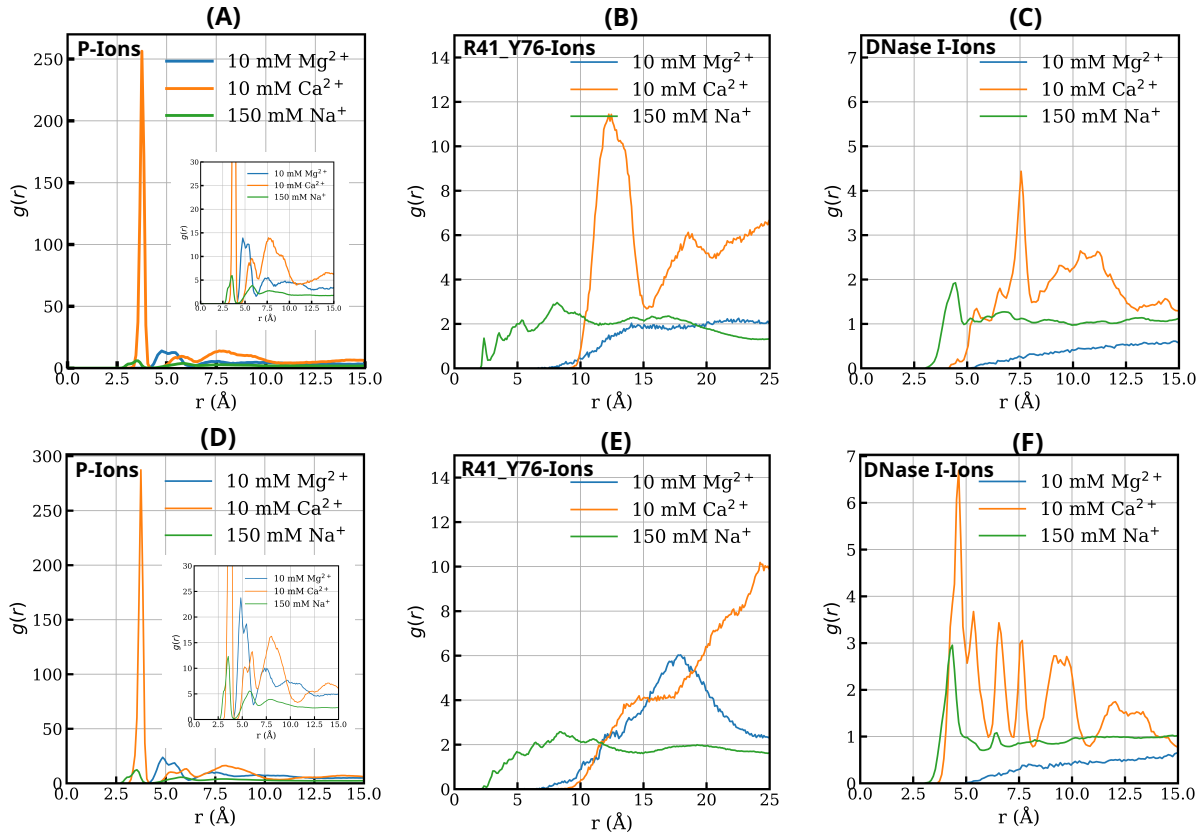

Figure S.7: Radial distribution functions, g(r), of the 10 mM divalent ions (Mg^{2+}/Ca^{2+}) and 150 mM of Na^{+} ions around DNA P and DNase I atoms, illustrating their roles in mediating DNA-DNase I binding. Panels (A-C) show g(r) between Mg^{2+}/Ca^{2+}/$^{+}$ ions and dsDNA P atoms, DNase I atoms, and DNase I active-site residue atoms, respectively, in the dsDNA-DNase I system. Panels (D-F) present the corresponding g(r) profiles between $Mg2^{2+}$/Ca^{2+}/Na^{+} ions and PX-DNA P atoms, DNase I atoms, and DNase I active-site residue atoms, respectively, in the PX-DNase I system.

A sharp first peak at short distances indicates close association and strong binding interactions between the divalent cations and DNA/DNase I atoms. As shown in Figure S.7A-C, at a concentration of 10 mM of Mg^{2+} and Ca^{2+} cations, Ca^{2+} ions exhibit a first sharp peak (orange color) at the shortest distance of ∼3.5 Å, indicating strong interactions with S.7(A) dsDNA, (B) DNase I, and (C) active-site residues (R41 and Y76). In contrast, the Mg^{2+} ions show a broader and weaker g(r) peak near ∼5Å, primarily near the dsDNA backbone, but do not show any sharp, distinct g(r) peaks near DNase I residues and DNase I backbone N atoms, clearly suggesting a more limited role in direct DNase I binding. Similar g(r) trends

are observed for the PX-DNase I system (Figure S.7D-F). Collectively, these results indicate that Ca^{2+} ions play a dominant role in mediating and bridging DNA-DNase I interactions through association with both the DNA duplex backbone and active-site residues, whereas Mg^{2+} ions preferentially associate with the DNA backbone alone.

S.5 Component-wise MMGBSA Binding Energy

Different energy component values of the time-averaged MMGSBA binding free energy from the final 50 ns of the 300 ns MD simulation trajectory

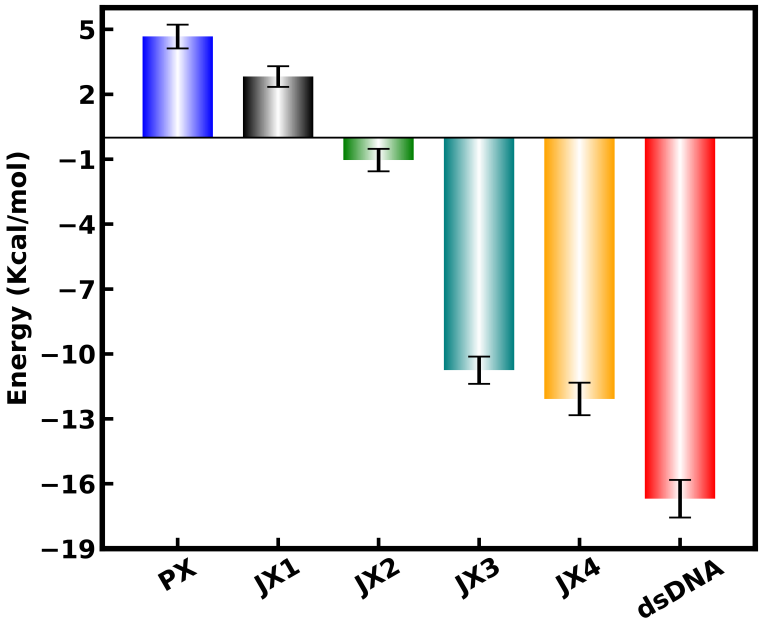

Figure S.8: Total MMGBSA binding energy for all six DNA-DNase I complexes at 300 K, from the equilibrium MD trajectory in the presence of 150 mM monovalent NaCl ions.

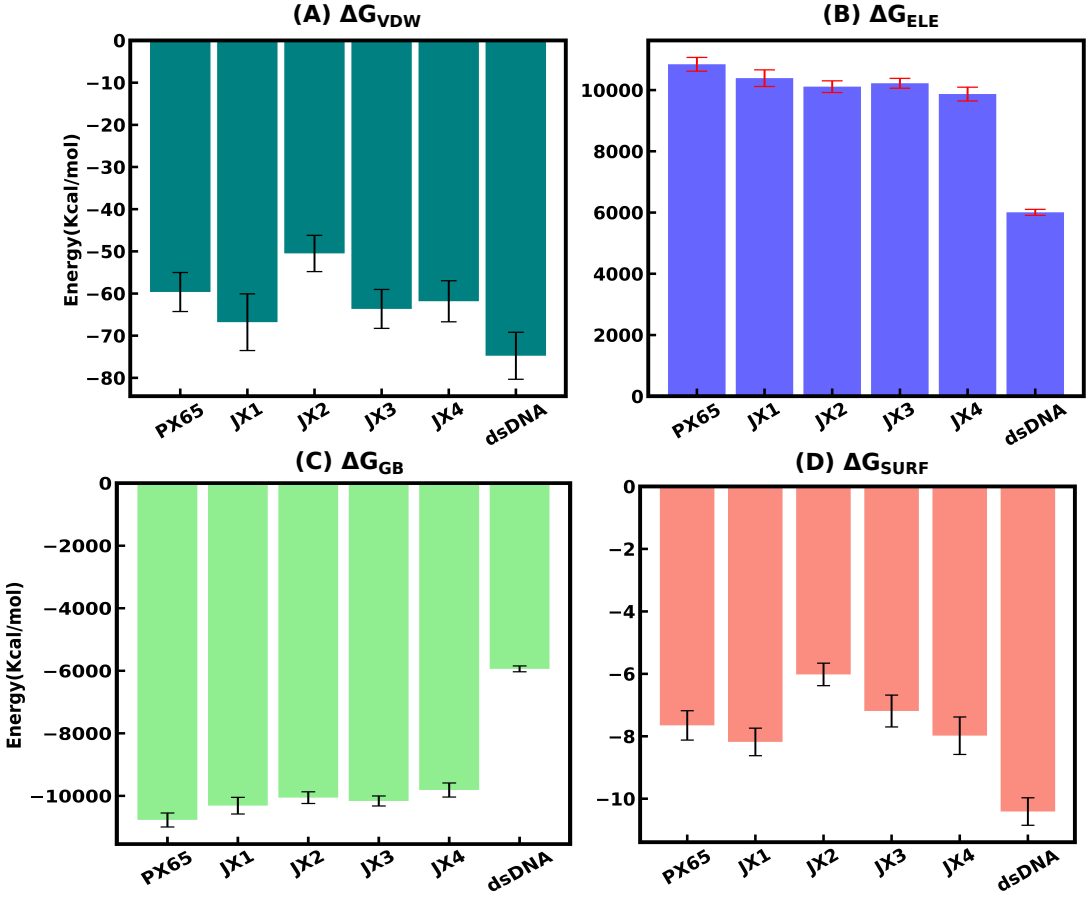

Figure S.9: MMGBSA binding energy is distributed into Electrostatic(ELE) energy, Born Solvation (GB) energy, Van der Waals (VDW) energy, and non-polar solvation-free energy (SURF) components as represented by (A-D), respectively, for all six DNA-DNase I complexes at 300 K, in the presence of 150 mM monovalent NaCl ions.

Table St.2: **Different energy components of binding free energy from MMGBSA analysis at 300 K using the final 50 ns from the 300 ns simulation trajectory in kcal/mol units, in the presence of 150 mM monovalent NaCl ions**

System	ΔE_{VDW}	ΔE_{ELE}	ΔE_{GB}	$\Delta G_{Binding\ Energy}$
PX	-59.65 ± 4.62	10841.81 ± 224.89	-10769.84 ± 223.04	**4.67 ± 0.35**
JX1	-66.80 ± 6.72	10390.60 ± 271.53	-10312.79 ± 267.27	2.82 ± 0.18
JX2	-50.50 ± 4.29	10111.04 ± 190.46	-10055.55 ± 187.99	-1.04 ± 0.22
JX3	-63.53 ± 4.87	10222.61 ± 161.28	-10162.64 ± 159.40	-10.75 ± 0.28
JX4	-61.84 ± 5.47	9869.37 ± 225.14	-9811.62 ± 224.41	-12.08 ± 0.23
dsDNA	-74.77 ± 5.11	6006.60 ± 96.52	-5938.11 ± 93.83	**-16.69 ± 0.27**

To quantitatively assess the DNA-DNase I interaction strength in the presence of divalent cations under physiological salt concentrations, we computed the binding free energies of the DNase I nuclease for both complexes using the MMGBSA approach, as summarized in Table St.3.

Table St.3: **Binding free energy components from MMGBSA analysis at 300 K using the final 50 ns from the 300 ns simulation trajectory in kcal/mol units, in the presence of 10 mM of divalent Mg^{2+} and Ca^{2+} ions.**

Energy Components (kcal/mol)	**dsDNA-DNase I (with divalent ions)**	**PX-DNA (with divalent ions)**
ΔE_{VDW}	-77.62±5.50	-49.02±4.70
ΔE_{ELE}	5316.25±120.22	10208.76±210.25
ΔE_{GB}	-5264.75±119.51	-10158.90±207.80
ΔE_{SURF}	-10.48±0.41	-7.20±0.41
$\Delta G_{Binding\ Energy}$	**-36.60±0.35**	**-6.36±0.30**

S.6 Free Energy Landscape for JX-DNA

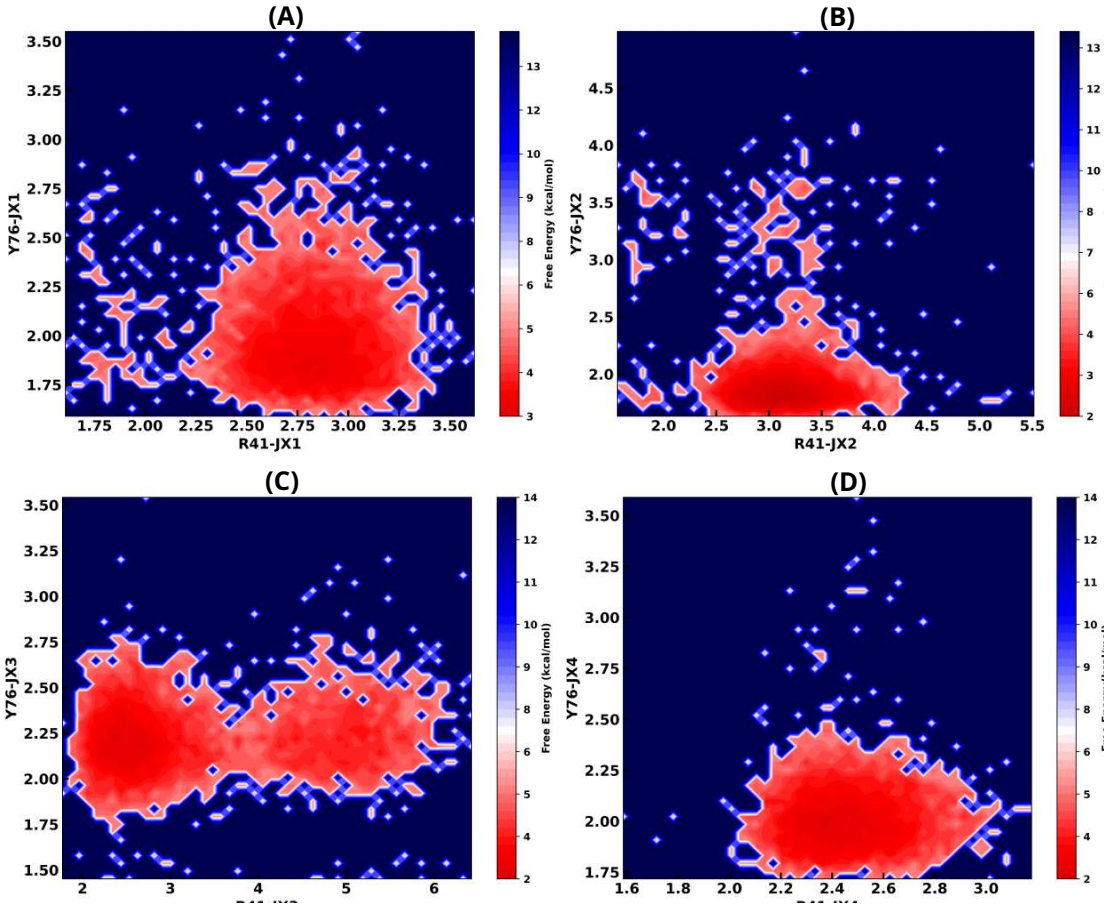

Figure S.10: Distance-based Free Energy Landscape (FEL) for the distance between binding sites of JX-DNA and active residues (R41 and Y76) of DNase I enzyme, as shown for (A) JX1, (B)JX2, (C)JX3 and (D) JX4, in the presence of 150 mM monovalent NaCl ions.

S.7 Contour Length Distributions of JX-DNA Nanostructures

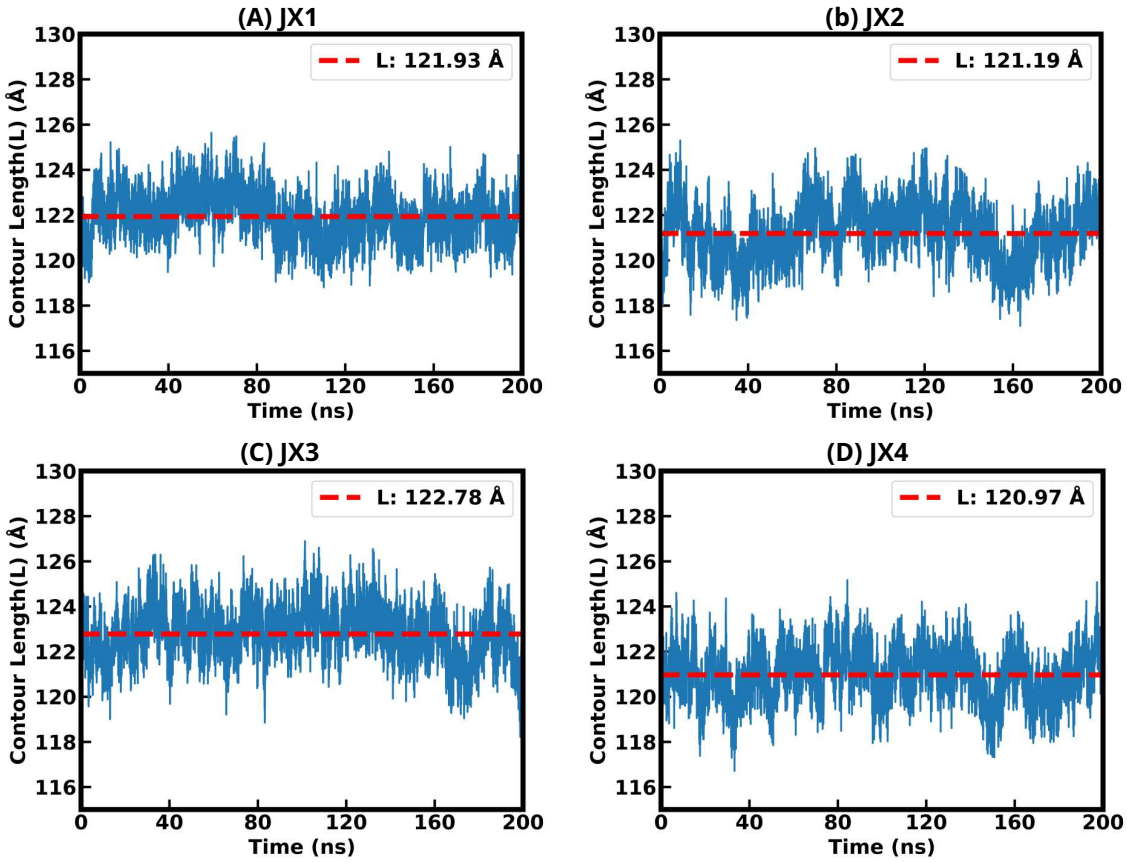

Figure S.11: Time evolution of contour length over the final 200 ns of the 300 ns all-atom MD simulations for the four JX–DNase I complexes at 300 K, shown in panels A–D, respectively, in presence of 150 mM monovalent NaCl ions.

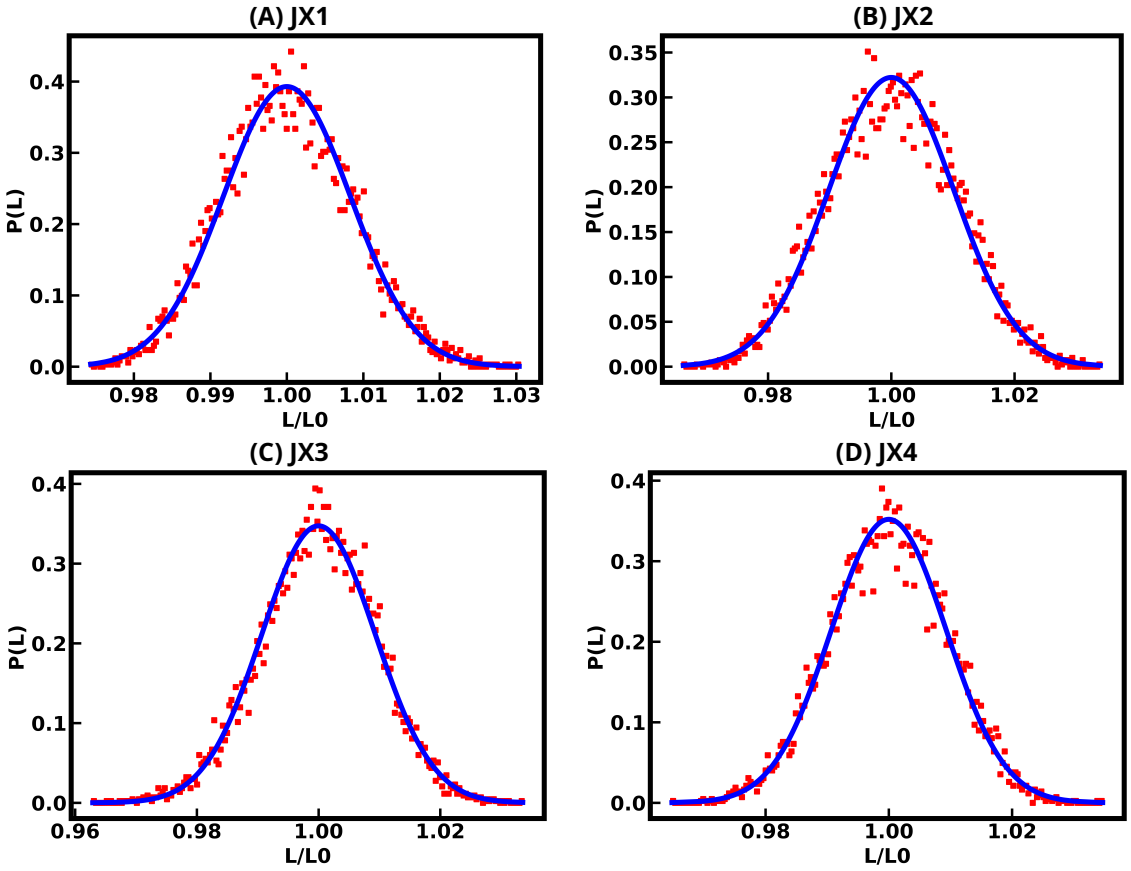

Figure S.12: Probability distributions of contour lengths derived from the final 200 ns of the 300 ns simulation trajectories for JX1, JX2, JX3, and JX4, upon DNase I binding, shown in panels A-D, respectively, at 300 K, in presence of 150 mM monovalent NaCl ions.

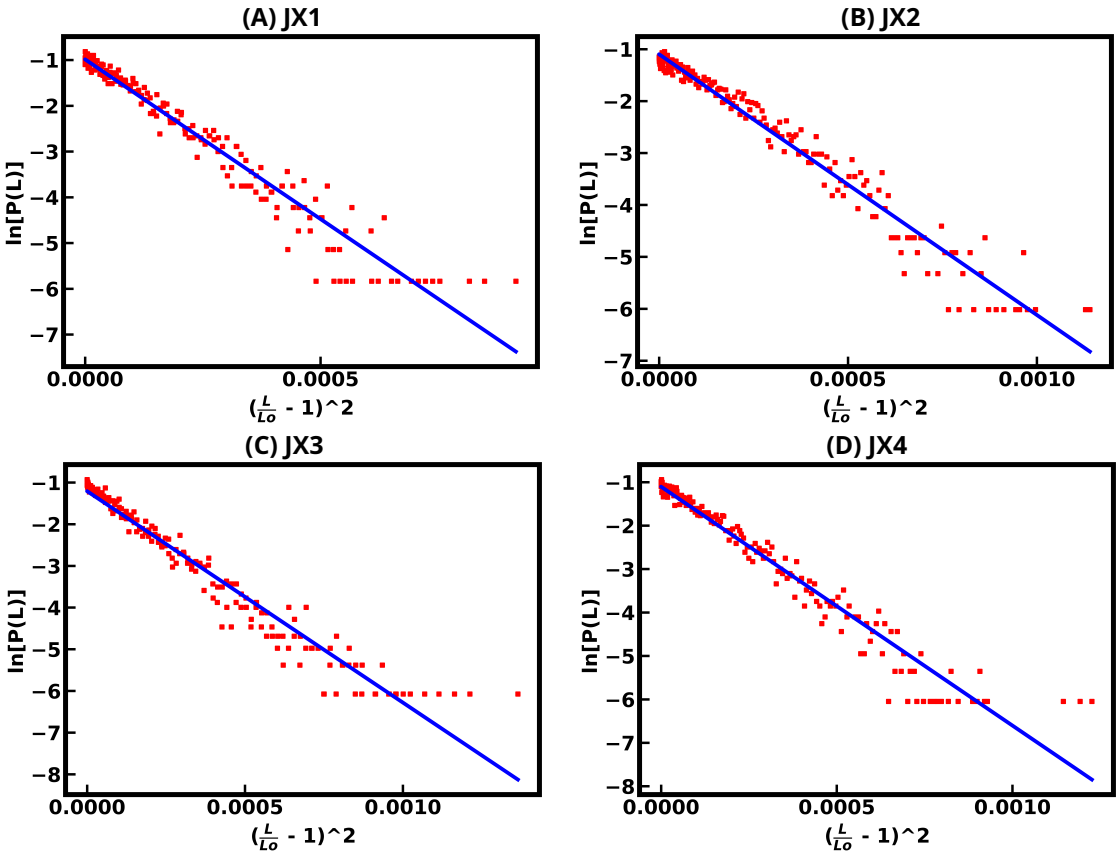

Figure S.13: Logarithmic fitting of the contour length distributions obtained from the final 200 ns of the 300 ns simulation trajectories for JX1, JX2, JX3, and JX4 nanostructures bound to DNase I, as shown in panels A-D, respectively, at 300 K, in presence of 150 mM monovalent NaCl ions.

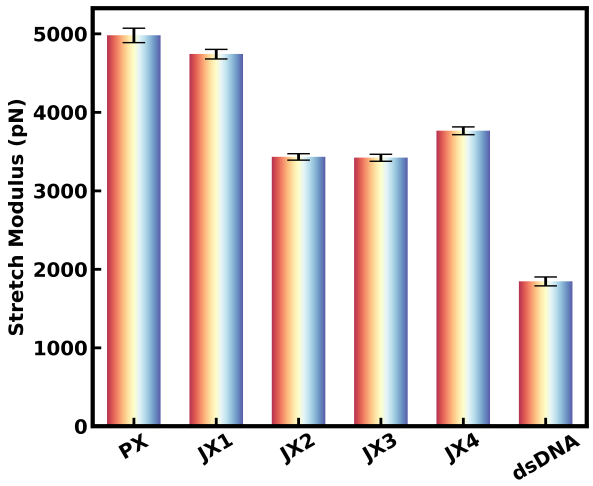

Figure S.14: Stretch modulus values of the four JX DNA nanostructures (JX1-JX4), derived from contour length distributions over the final 200 ns of the 300 ns MD simulation trajectories, reveal their relative flexibility upon binding of the DNase I enzyme, in presence of 150 mM monovalent NaCl ions.

Table St.4: **Mechanical Properties of native dsDNA, JX's (JX1-JX4) and PX-DNA nanostructures using contour length distribution from the last 200 ns all-atom simulation trajectory at 300 K and the Helical parameters (MGW and Twist), in presence of 150 mM monovalent NaCl ions.**

System details	Contour Length(L_0) (Å)	MGW (Å)	Twist (Degree)	Stretch Modulus(γ_G) (pN)
PX-DNA	125.64 ± 0.62	10.21 ± 4.44	35.85 ± 0.37	4804.54 ± 87.83
JX1	121.93 ± 0.68	10.79 ± 4.37	33.87 ± 0.32	4741.86 ± 61.06
JX2	121.18 ± 0.83	10.41 ± 4.20	33.70 ± 0.28	3432.33 ± 41.13
JX3	122.77 ± 0.77	11.23 ± 4.65	34.80 ± 0.38	3421.24 ± 44.17
JX4	120.96 ± 0.76	10.88 ± 4.02	33.33 ± 0.41	3765.23 ± 50.02
dsDNA	118.97 ± 1.03	11.54 ± 4.05	32.66 ± 0.78	1845.39 ± 56.99

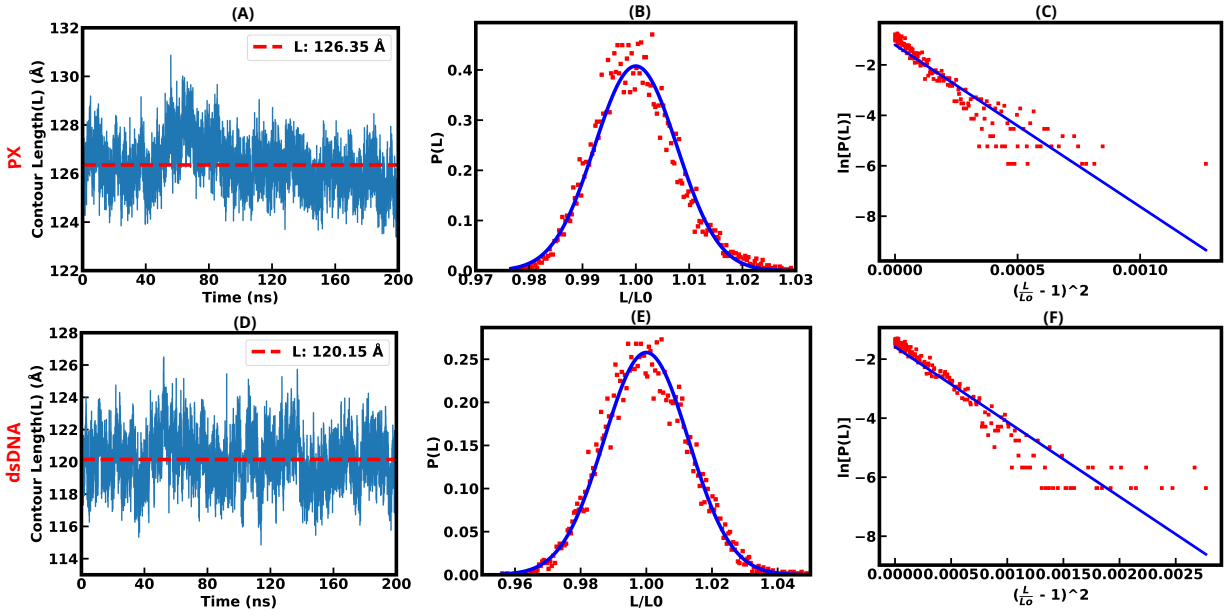

Figure S.15: Stretch modulus of PX and dsDNA nanostructures in the presence of 10 mM divalent cations (Mg^{2+}/Ca^{2+}), derived from contour length distributions over the final 200 ns of the 300 ns MD simulation trajectories, reveals their relative flexibility upon binding of the DNase I enzyme.

Table St.5: **Mechanical Properties of native dsDNA, and PX-DNA nanostructures using contour length distribution from the last 200 ns all-atom simulation trajectory at 300 K, in presence of 10 mM divalent Mg^{2+} and Ca^{2+} cations.**

System details	Contour Length(L_0) (Å)	MGW (Å)	Twist (Degree)	Stretch Modulus(γ_G) (pN)
PX	126.35 ± 0.66	10.86 ± 4.80	34.81 ± 0.28	4206.28 ± 90.95
dsDNA	120.15 ± 1.04	10.69 ± 4.64	33.05 ± 0.50	1749.53 ± 34.31

Table St.6: **Stretch modulus (γ_G) values of dsDNA and PX-DNA under different ionic conditions.**

System	Salt concentration (mM)	Stretch modulus γ_G (pN)
dsDNA	150 mM Na^+	1845.39 ± 56.99
	150 mM Na^+ + 10 mM Mg^{2+} + 10 mM Ca^{2+}	1749.53 ± 34.31
PX-DNA	150 mM Na^+	4804.54 ± 87.83
	150 mM Na^+ + 10 mM Mg^{2+} + 10 mM Ca^{2+}	4206.28 ± 90.95